

Electronic Supplementary Information

For

Strong Two-Photon Induced Phosphorescent Golgi-Specific In-Vitro Marker Based on a Heteroleptic Iridium Complex

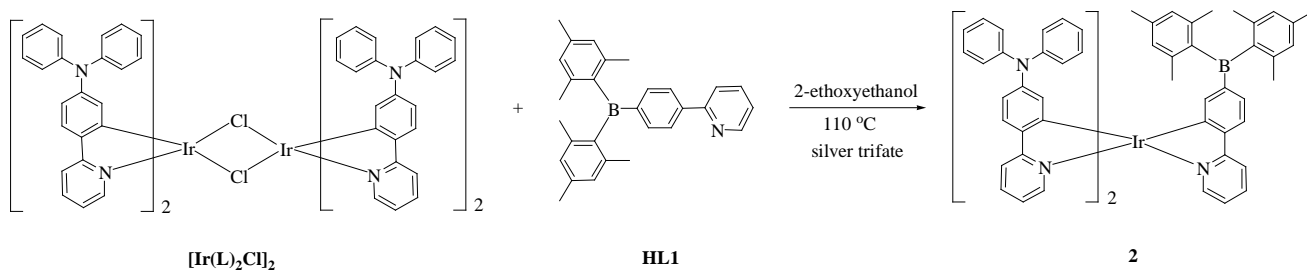
Cheuk-Lam Ho*, Ka-Leung Wong, Hoi-Kuan Kong, Yu-Man Ho, Chris Tsz-Leung Chan, Wai-Ming Kwok, Kelvin Sze-Yin Leung, Hoi-Lam Tam, Michael Hon-Wah Lam, Xue-Feng Ren, Ai-Min Ren, Ji-Kang Feng, and Wai-Yeung Wong*

Experimental Section

Synthesis: Preparation of **HL**, **HL1** and **1** was reported in the literature (Ref. *Adv. Funct. Mater.*, 2008, **18**, 499–511 and *Chem. Asian J.*, 2008, **3**, 1830–1841).

Synthesis of 2: $[\text{Ir}(\text{L})_2\text{Cl}]_2$ (240 mg, 0.137 mmol) and **HL1** (236 mg, 0.587 mmol) were dissolved in 8 mL of 2-ethoxyethanol and AgOTf (75.1 mg, 0.292 mmol) was added. The mixture was allowed to reflux at 110 °C for two days. After the solution was cooled down, the mixture was filtered and was extracted with dichloromethane and brine several times. The combined organic layer was evaporated to dryness to yield an orange oily residue. This residue was purified on TLC plates using dichloromethane as eluent to yield a bright orange product (17 mg, 10%). A sample of very high purity was obtained by chromatographic separation from its neighbouring minor components. In brief, the solid residue was dissolved in a minimal amount of methanol, and the solution was filtered and subject to HPLC separation. An Agilent 1100 HPLC system including a quaternary pump and a vacuum degasser was used. The column configuration consisted of a guard column and C₈ column (Alltima, 250 × 4.6 mm, 10 μm). The mobile phase consisted of 100% acetonitrile. The flow rate was 0.7 mL/min with an injection volume of 50 μL; the column was kept at 25°C. The DAD detector was set at the optimum wavelength of 395 nm. Compound **2** was found baseline separated from other minor peaks.

¹H NMR (CDCl₃): δ [ppm] 8.80 (m, 1H, Ar), 8.65–7.87 (m, 9H, Ar), 7.45–7.20 (m, 3H, Ar), 7.12 (m, 8H, Ar), 6.96 (m, 13H, Ar), 6.60 (m, 9H, Ar), 6.21 (m, 2H, Ar), 2.21 (s, 6H, CH₃), 1.67 (s, 12H, CH₃); MALDI-TOF MS: *m/z* 1237.4793 (calc. M⁺: 1237.4817, error = 2.0202 ppm); elemental analysis calcd (%) for C₇₅H₆₃N₅Bi: C 72.80, H 5.13, N 5.66; found: C 72.62, H 5.05, N 5.43



Spectroscopic and photophysical measurements: UV-Visible absorption spectra in the spectral range 200 to 1100 nm were recorded by a HP UV-8453 spectrophotometer. Single-photon luminescence spectra were recorded using a Edinburgh Instrument FLS920 Combined Fluorescence Lifetime and Steady state spectrophotometer that was equipped with a red-sensitive single-photon counting photomultiplier in Peltier Cooled Housing. The spectra were corrected for detector response and stray background light phosphorescence. The luminescence quantum yield is 0.12 in aqueous solution (5%

DMSO). The experimental details for quantum yield measurements are shown below. The emission spectra were recorded in an integrated sphere on a FLS-920 (Demountable 142 mm (inner) diameter barium sulfate-coated integrating sphere supplied with two access ports in Edinburgh Instrument FLS920 with a Hamamatsu R928 detector. The quantum yield was estimated by the equation developed by de Mello et al. (J. C. de Mello, H. F. Wittmann and R. H. Friend, *Adv. Mater.*, 1997, **9**, 230.)

$$QY = (E_{\text{Indirect}}L_{\text{direct}}) - (E_{\text{direct}}L_{\text{indirect}}) / (E_{\text{Indirect}}E_{\text{without}}) - (E_{\text{direct}}L_{\text{without}}) \quad (1)$$

E – spectrum of the light (scattering) used to excite the sample (where direct is the light passing through the sample and indirect is without the sample in the sphere)

L – emission spectrum of the sample collected using the sphere

The phosphorescence lifetime of complex **2** is 0.47 μs in aqueous solution and the emission lifetime was monitored by the FLSP-920 (equipped with NF900 nanosecond flash lamp for ps to 10 μs lifetime measurement).

Two-photon induced emission measurements: For two-photon experiments, the 730 nm pump source was from the fundamental of a femtosecond mode-locked Ti:Sapphire laser system (output beam ~ 150 fs duration and 1 kHz repetition rate). The 700–900 nm pump wavelengths were generated from a commercial optical parametric amplifier (Coherent) pumped by the SHG of the 800 nm femtosecond pulses. The laser beam was focused to a spot size ~ 50 μm via an $f = 10$ cm lens onto the sample. The emitting light was collected with a backscattering configuration into a 0.5 m spectrograph and detected by a liquid nitrogen-cooled CCD detector. A power meter was used to monitor the uniform excitation.

Two-photon absorption cross-section measurements: The theoretical framework and experimental protocol for the two-photon cross-section measurement have been outlined by Webb and Xu (Ref. C. Xu and W. W. Webb, *J. Opt. Soc. Am. B*, 1996, **13**, 481–489). In this approach, the two-photon excitation (TPE) ratios of the reference and sample systems are given by:

$$\frac{\sigma_2^S \cdot \phi^S}{\sigma_2^R \cdot \phi^R} = \frac{C_R \cdot n_S \cdot F^S(\lambda)}{C_S \cdot n_R \cdot F^R(\lambda)}$$

where ϕ is the quantum yield, C is the concentration, n is the refractive index, and $F(\lambda)$ is the integrated photoluminescent spectrum. In our measurements, we have ensured that the excitation flux and the excitation wavelengths are the same for both the sample and the reference. The two-photon absorption cross-section σ of complexes **1** and **2** were determined using Rhodamine 6G as a reference.

Microscopy imaging: To study the localization behaviour of the iridium complexes, experiments were

carried out in a multi-photon confocal microscopy. For the two-photon *in-vitro* imaging, the cells were imaged in a tissue culture chamber (5% CO₂, 37 °C) using a Leica SP5 (upright configuration) confocal microscope equipped with a femtosecond-pulsed Ti:Sapphire laser (Libra II, Coherent). The excitation beam produced by the femtosecond laser, which was tunable from 720–900 nm, ($\lambda_{\text{ex}} = 800 \text{ nm}$, $\sim 3 \text{ mW}$), passed through an LSM 510 microscope with HFT 650 dichroic (Carl Zeiss, Inc.) and focused on coverslip-adherent cells using a 63 x oil immersion objective. Red Golgi tracker (Invitrogen, Alexa Fluor 647) was used for co-staining with our iridium complex **2** ($\lambda_{\text{ex}} = 647 \text{ nm}$, $\lambda_{\text{em}} = \sim 655\text{-}750 \text{ nm}$). The co-staining experiment was done under two-photon excitation to prevent the excitation of the commercial red Golgi tracker.

Cell culture: Human lung carcinoma A549 cells were purchased from the American type Culture Collection (ATCC) (#CCL-185, ATCC, Manassas, VA, USA). Cells were cultured in Ham's F12K medium with L-glutamine and phenol red (N3520, Sigma, St. Louis, MO, USA) supplemented with 10% fetal bovine serum (FBS) at 37 °C and 5% CO₂. Cells were passaged every 3–5 days. Human cervical carcinoma (HeLa) cells were maintained in RPMI 1640 medium supplemented with 10% FBS and 1% penicillin and streptomycin in 5% CO₂.

3-(4,5-Dimethyl thiazol-2-yl)-2,5-diphenyl tetrazolium bromide assay (cytotoxicity assay). Cell viability was measured using the 3-(4,5-dimethylthiazol-2-yl)-2,5-diphenyltetrazolium bromide (MTT) proliferation assay. Briefly, HeLa cells were seeded in a 96-well flat-bottomed microplate (6000 cells/well) and cultured in 100 μL growth medium at 37 °C and 5% CO₂ for 24 h. Cell culture medium in each well was then replaced by 100 μL DMSO-charged cell growth medium (max. 1:99, v/v), which contained the iridium complex at concentrations ranging from 10⁻⁷ to 10⁻⁴ M. After incubation for 20 h, 20 μL MTT labeling reagent (5 mg/mL in PBS solution) was added to each well for further 4 h incubation at 37 °C. The growth medium was removed gently by suction, and 200 μL DMSO was then added to every well as the solubilizing agent, sitting at room temperature overnight to dissolve the formazan crystals completely. The absorbance at the wavelength of 570 nm was measured by Multiskan EX (Thermo Electron Corporation), and each data point was represented as means \pm SD from triplicate wells. (Ref: A. P. Wilson, *Cytotoxicity and Viability Assays in Animal Cell Culture: A Practical Approach*, 3rd ed. (ed. J. R. W. Masters), Oxford University Press: Oxford, 2000, Vol.1)

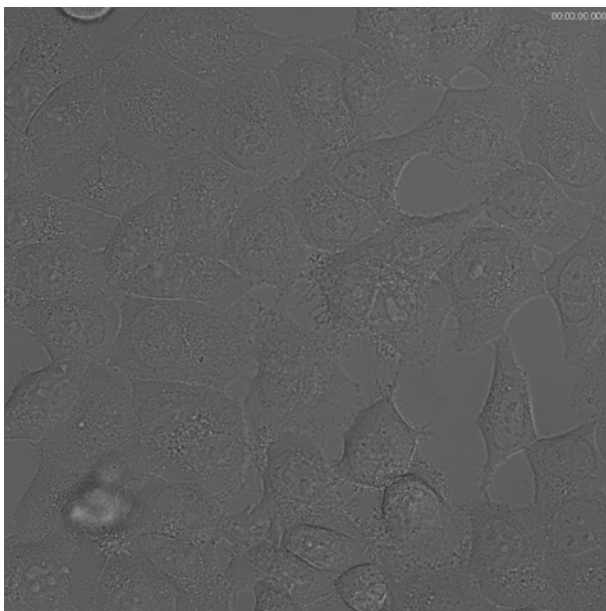


Figure S1. The bright field image for Figure 2.

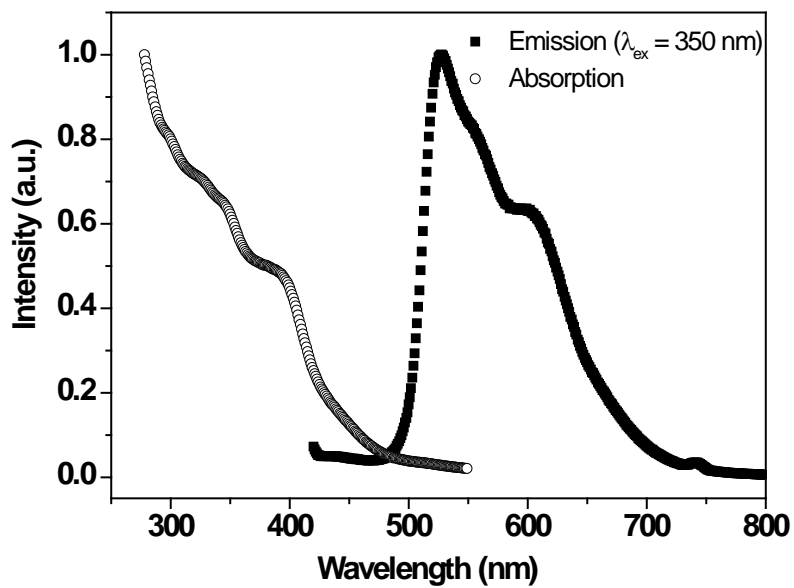


Figure S2. The absorption and emission spectra of complex 2 in DMSO (10^{-4} M).

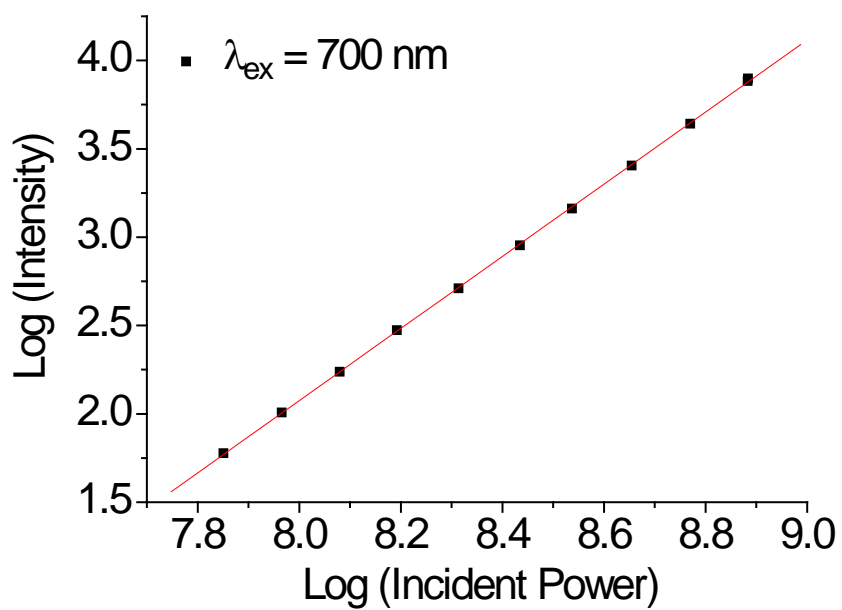


Figure S3. Power dependence experiment of complex 2 ($\lambda_{\text{ex}} = 700 \text{ nm}$ and $\lambda_{\text{em}} = 530 \text{ nm}$)

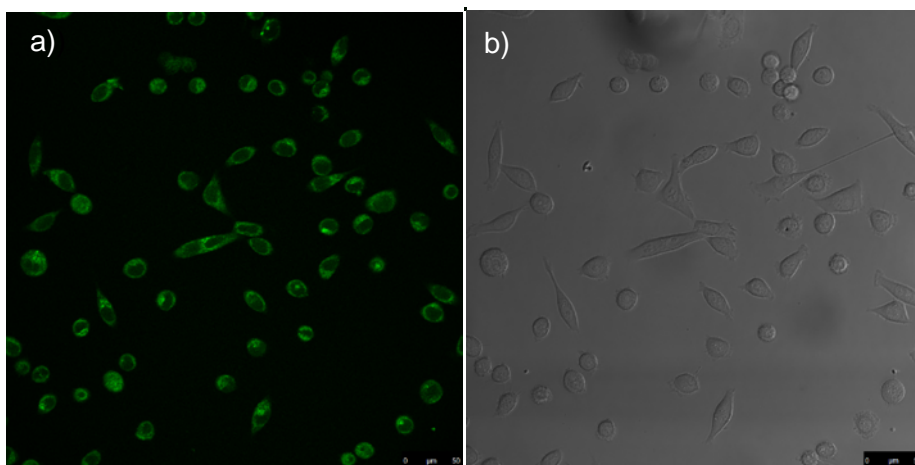


Figure S4. *In-vitro* microscopy with complex 1 ($\lambda_{\text{ex}} = 700 \text{ nm}$, HeLa; a): 45 min, b) is the bright field image of panel a) for 6 h).

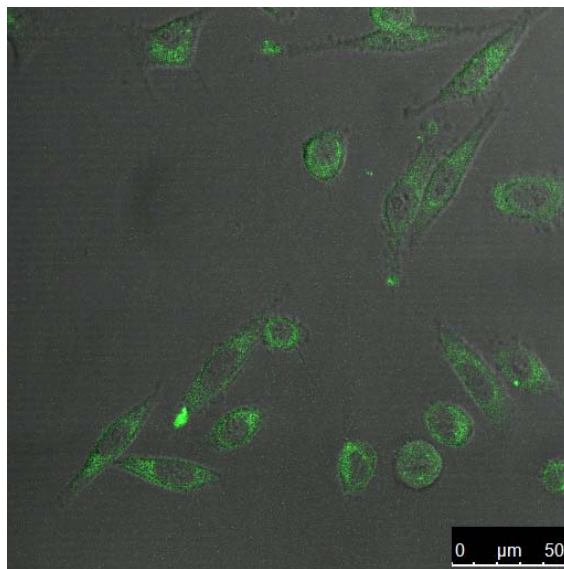


Figure S5. *In-vitro* microscopy with complex **2** ($\lambda_{\text{ex}} = 700 \text{ nm}$, HeLa; after a dosage time of 7 h).

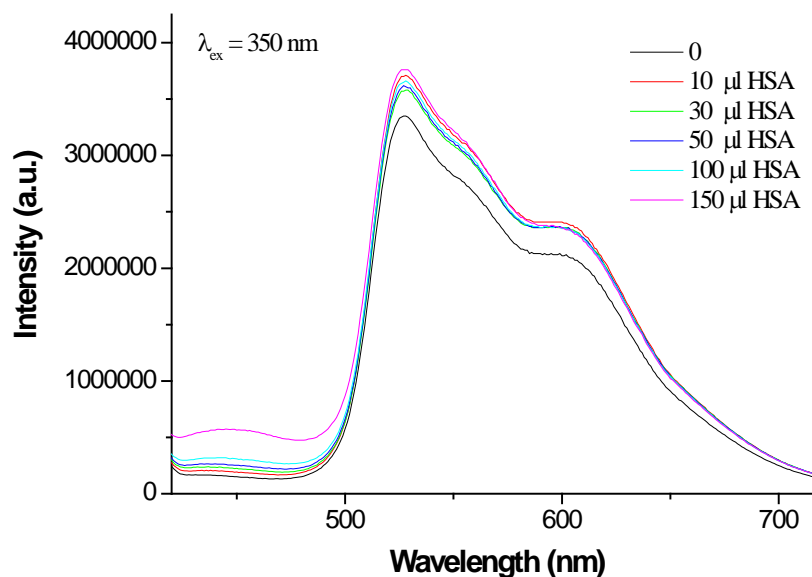


Figure S6. The titration experiments of complex **2** with various concentrations (10 – 150 μL) of HAS.

Computational details

Density functional theory (DFT) method with B3LYP approach was employed to optimize the ground-state geometries of compounds **1** and **2**. The energies of the excited singlet states of these compounds were computed by time-dependent (TD) B3LYP based on all the ground-state optimization geometries. In the calculations, the effective core potentials (LANL2DZ) were adopted for Ir atom, and the 6-31G(d) basis set for the non-metal atoms (H, C, N and B).

Frontier molecular orbital properties: The frontier molecular orbitals energies and compositions of compounds **1** and **2** are drawn in Figure S7. Figure S7 shows the calculated HOMO energies of compounds **1** and **2** decrease as $-4.54 > -4.58$ eV, while their LUMO energies decrease as $-1.14 > -1.69$ eV in the same order. Obviously, adding the efficient electron-withdrawing mesitylborane group is an effective way of decreasing the LUMO energy, which indicates the electron accepting ability of compound **2** is improved relative to **1**.

Figure S7 also shows the occupied molecular orbitals, HOMO, HOMO-1, HOMO-2 of compound **1** are dominantly located on the ligands. While for its HOMO-3, HOMO-4, and HOMO-5, the contribution of 5d orbital from Ir center is decreased to 46.9% dz^2 , 25.3% dxy , 25% dx^2-y^2 , respectively. With the introduction of a mesitylborane group in **2**, the molecular orbital compositions are similar to those of compound **1**. The occupied molecular orbitals, HOMO, HOMO-1 of compound **2** are mainly located on the ligands, while the HOMO-2, HOMO-3, HOMO-4 has obvious metal contributions.

Electronic absorption spectra: The calculated singlet excited states of compounds **1** and **2** are tabulated in Table S1, together with their oscillator strengths, main configurations and assignments.

As listed in Table S1, the lowest lying distinguishable absorption peaks of compounds **1** and **2** are located at 434.6 and 508.8 nm, respectively. Based on the analysis of molecular orbital composition (shown in Figure S7), the absorption peaks at 434.6 and 508.8 nm of compounds **1** and **2** can be ascribed to the mixed LLCT/ILCT and LLCT, respectively.

In addition, another distinguished absorption bands for compound **1** are at 416.5 and 416.4 nm, which can be described as LLCT/ILCT transition character. The calculated absorptions at 390.8 and 371.9 nm of compound **1** are assigned to mixed MLCT/LLCT/ILCT characters. For compound **2**, the calculated absorption bands of 434.5 and 428.0 nm arising from S_5 and S_7 possess mixed transition character of LLCT/ILCT associated with minor MLCT character. Similarly, the S_{22} of compound **2** is assigned to ILCT character.

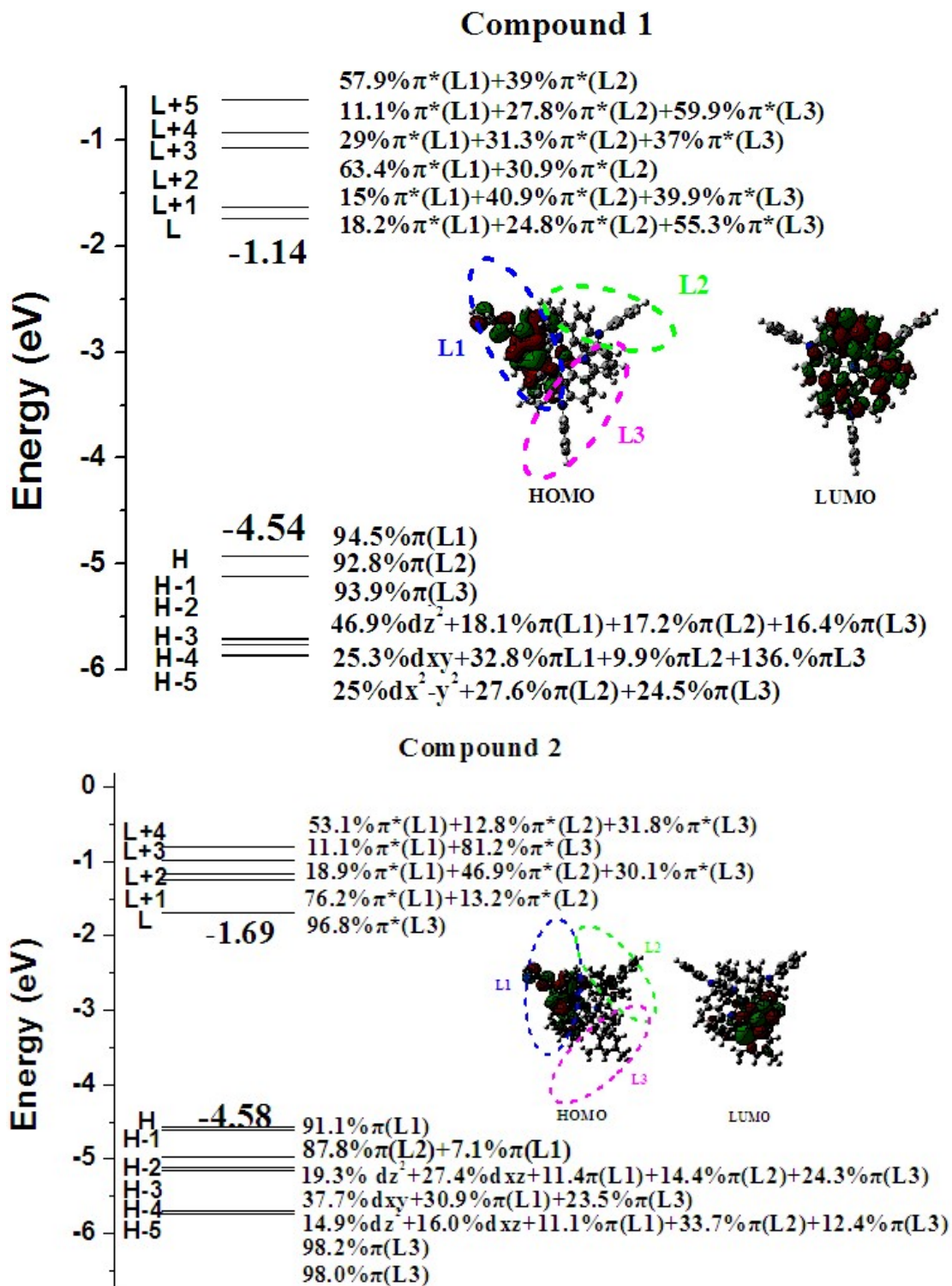


Figure S7. The energies (eV), partial molecular orbital compositions (%) for compounds **1** and **2** together with the electron density distributions of their HOMO and LUMO.

Table S1. Computed electronic transitions of **1** and **2**.

	$\lambda(\text{nm})$	Oscillator strength	Configuration	Assignment
Compound 1				
S ₁	434.6	0.0611	H→L(72%)	LLCT/ILCT
S ₄	416.5	0.0905	H-2→L(52%)	LLCT/ILCT
S ₅	416.4	0.0884	H-1→L(52%)	LLCT/ILCT
S ₁₀	390.8	0.0962	H-3→L(61%)	MLCT/LLCT/ILCT
S ₁₈	372.9	0.0898	H-4→L+2(33%)	MLCT/LLCT/ILCT
			H-5→L+1(33%)	MLCT/LLCT/ILCT
S ₂₂	356.1	0.0773	H→L+4(71%)	LLCT/ILCT
S ₂₃	355.9	0.0781	H→L+5(70%)	LLCT/ILCT
S ₂₄	352.8	0.0792	H-2→L+4(42%)	LLCT/ILCT
			H-1→L+5(41%)	LLCT/ILCT
Compound 2				
S ₁	508.8	0.0019	H→L(87%)	LLCT
S ₅	434.5	0.1116	H-1→L+1(46%)	LLCT/ILCT
S ₇	428.0	0.1396	H→L+1(33%)	LLCT
			H-2→L+1(26%)	MLCT/LLCT/ILCT
S ₉	416.2	0.0807	H→L+2(46%)	LLCT/ILCT
S ₁₀	405.9	0.1123	H-2→L+1(63%)	MLCT/LLCT/ILCT
S ₂₀	367.7	0.0645	H→L+4(46%)	LLCT/ILCT
S ₂₁	365.0	0.0761	H-1→L+4(30%)	LLCT/ILCT
S ₂₂	360.6	0.1065	H-6→L(79%)	ILCT

Table S2. Photophysical data of **1** and **2** in DMSO.

	Φ	$\tau(\mu\text{s})$
1	0.21	0.28
2	0.19	0.35

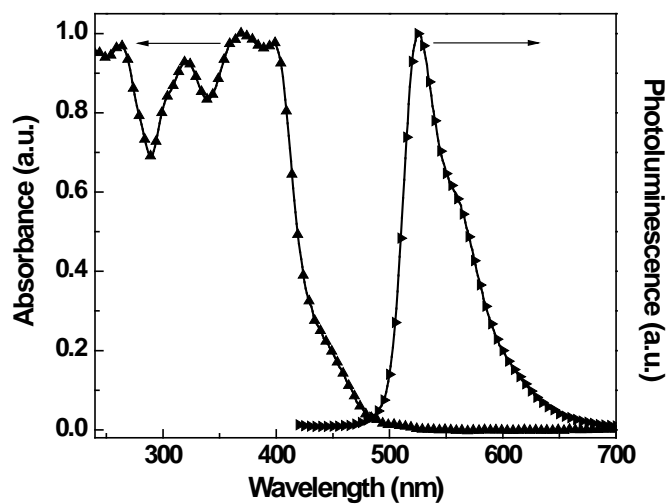


Figure S8. Absorption and emission spectra of **1** in CH₂Cl₂.

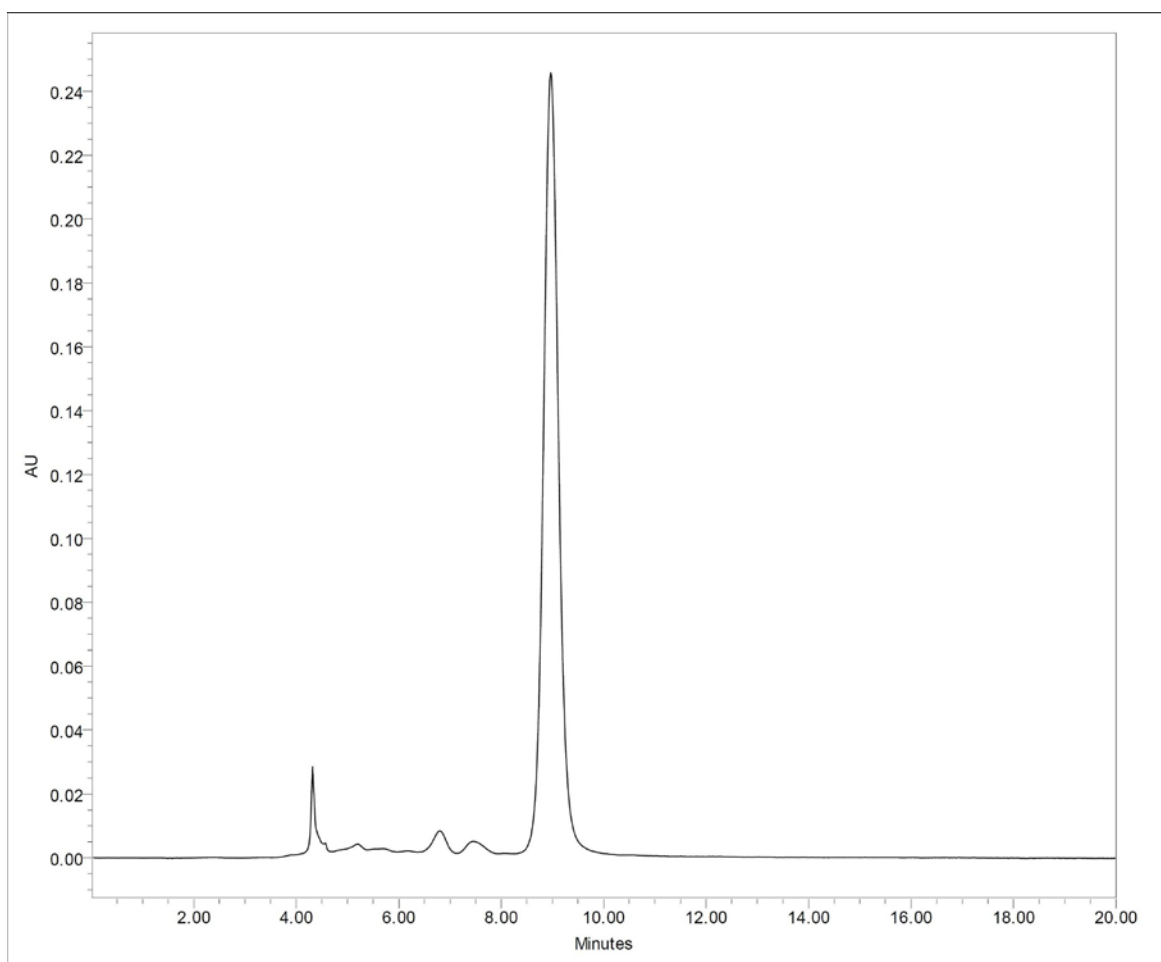


Figure S9. HPLC chromatogram for purifying the sample of compound **2** (the strongest peak).

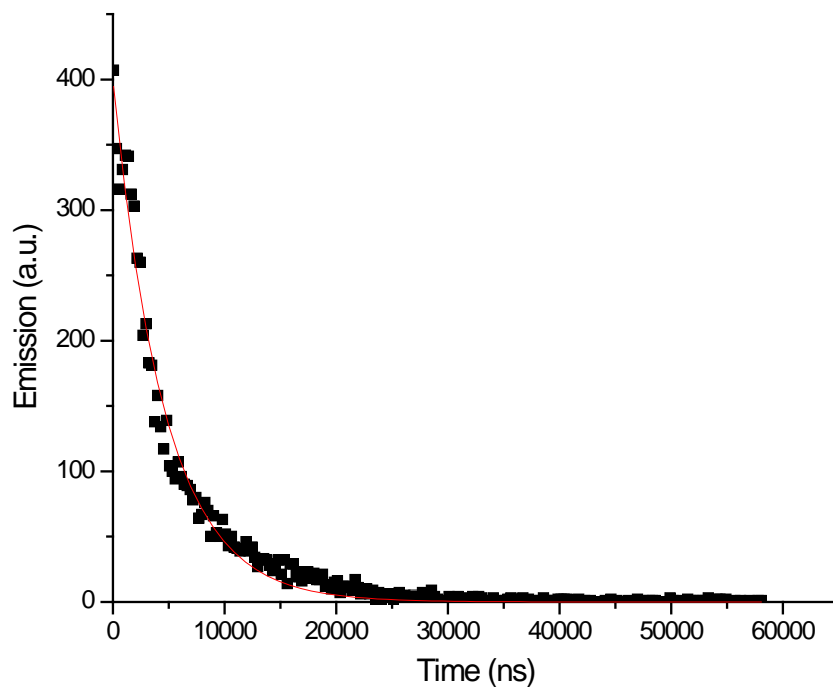


Figure S10. The emission decay curve of **2** measured in DMSO (0.1 mM, $\lambda_{\text{ex}} = 350$ nm; $\lambda_{\text{em}} = 520$ nm).

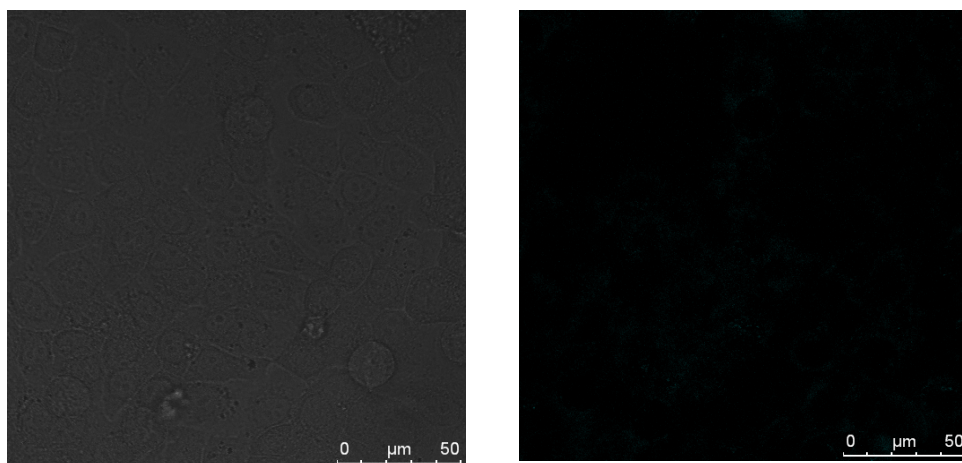


Figure S11. The *in-vitro* imaging of DMSO was monitored in HeLa (same experimental conditions, i.e. laser power and excitation wavelength as in Figure 2) as control experiments (3% DMSO, $\lambda_{\text{ex}} = 350$ nm; $\lambda_{\text{em}} = 520$ nm).

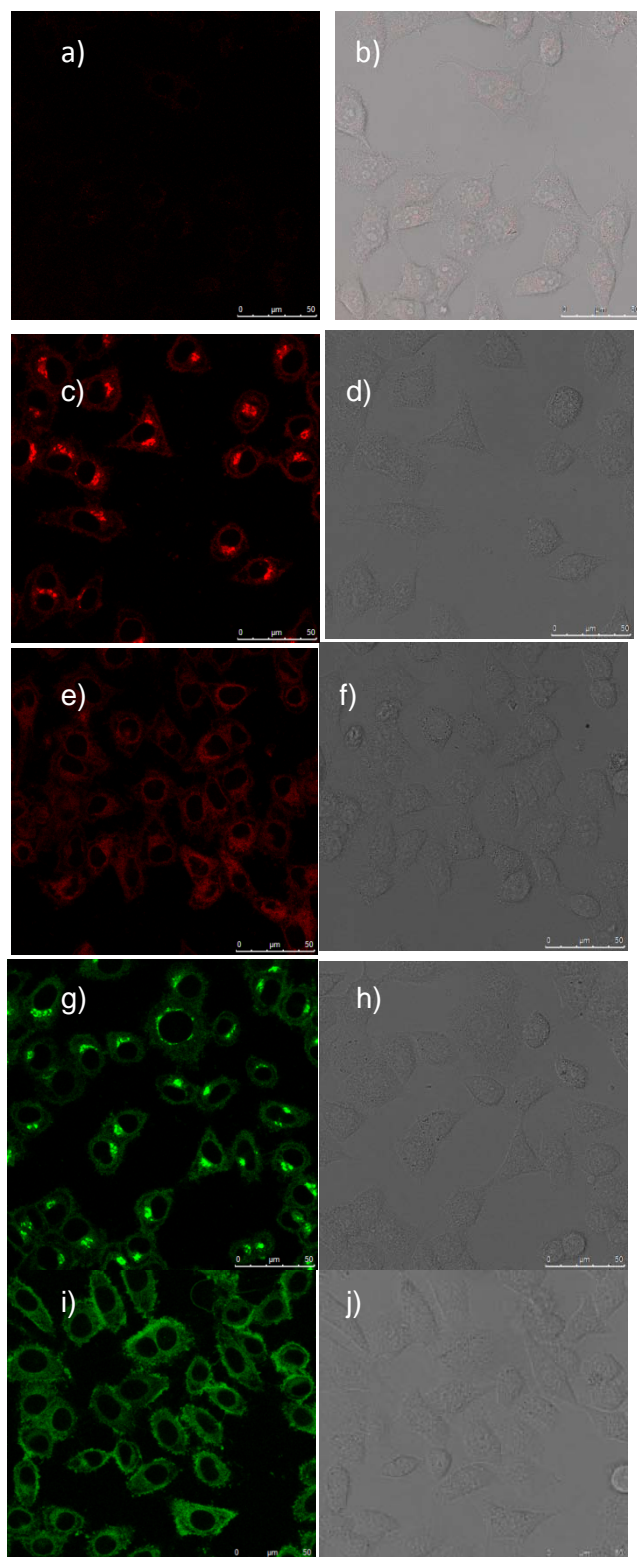


Figure S12. Negative control experiments designed to further confirm the complex **2** as Golgi specific marker. (a-b) In-vitro image of HeLa cells treated with 1 mg/mL Brefeldin A (BFA) for 30 min and their bright field images; (c-f) HeLa cells treated with commercial Golgi marker Alexa Fluor 647 conjugates (1 μ M, Invitrogen L32452) without (c and d) and with (e and f) 1 mg/mL Golgi inhibitor Brefeldin A for 30 min; (g-j) HeLa cells treated with complex **2** (1 μ M) for 30 min without (g and h) and with (i and j) 1 mg/mL Golgi inhibitor Brefeldin A for 30 min.